

Histone H4 Hyperacetylation Precludes Histone H4 Lysine 20 Trimethylation*

Received for publication, August 9, 2004, and in revised form, September 23, 2004
Published, JBC Papers in Press, September 28, 2004, DOI 10.1074/jbc.M409099200

Bettina Sarg^{‡§}, Wilfried Helliger^{‡§}, Heribert Talasz[‡], Elisavet Koutzamani[¶],
and Herbert H. Lindner^{‡||}

From the [‡]Department of Medical Chemistry and Biochemistry, Medical University of Innsbruck, Fritz-Pregl-Strasse 3, A-6020 Innsbruck, Austria and [¶]Department of Biomedicine and Surgery, Division of Cell Biology, Faculty of Health Sciences, Linköpings Universitet, SE-581 85 Linköping, Sweden

Posttranslational modification of histones is a common means of regulating chromatin structure and thus diverse nuclear processes. Using a hydrophilic interaction liquid chromatographic separation method in combination with mass spectrometric analysis, the present study investigated the alterations in histone H4 methylation/acetylation status and the interplay between H4 methylation and acetylation during *in vitro* differentiation of mouse erythroleukemia cells and how these modifications affect the chromatin structure. Independently of the type of inducer used (dimethyl sulfoxide, hexamethylenbisacetamide, butyrate, and trichostatin A), we observed a strong increase in non- and monoacetylated H4 lysine 20 (H4-Lys²⁰) trimethylation. An increase in H4-Lys²⁰ trimethylation, however, to a clearly lesser extent, was also found when cells accumulated in the stationary phase. Since we show that trimethylated H4-Lys²⁰ is localized to heterochromatin, the increase in H4-Lys²⁰ trimethylation observed indicates an accumulation of chromatin-dense and transcriptionally silent regions during differentiation and during the accumulation of control cells in the stationary phase, respectively. When using the deacetylase inhibitors butyrate or trichostatin A, we found that H4 hyperacetylation prevents H4-Lys²⁰ trimethylation, but not mono- or dimethylation, and that the nonacetylated unmethylated H4-Lys²⁰ is therefore the most suitable substrate for H4-Lys²⁰ trimethylase. Summarizing, histone H4-Lys²⁰ hypotrimethylation correlates with H4 hyperacetylation and H4-Lys²⁰ hypertrimethylation correlates with H4 hypoacetylation. The results provide a model for how transcriptionally active euchromatin might be converted to the compacted, transcriptionally silent heterochromatin.

In eukaryotes, histone proteins associate with DNA to form nucleosomes that are folded into higher order chromatin structures. Differences in higher order chromatin structures, which are important prerequisites for numerous biological processes including cellular proliferation, differentiation, development, gene expression, genome stability, and cancer, are thought to be realized by a variety of posttranslational modifications of

histone N termini, particularly of histones H3 and H4. Besides acetylation, histones are subjected to phosphorylation, methylation, ubiquitination, ADP-ribosylation, and deamidation (1, 2). Distinct combinations of covalent histone modifications including lysine acetylation, lysine and arginine methylation, and serine phosphorylation form the basis of the histone code hypothesis (3–5). This hypothesis proposes that a pre-existing modification affects subsequent modifications on histone tails and that these modifications generate unique surfaces for the binding of various proteins or protein complexes responsible for higher order chromatin organization and gene activation and inactivation. Some of the histone-modifying enzymes (*e.g.* lysine methyltransferases) are, when deregulated, considered to be involved in carcinogenesis (6).

Histone H4 is typically acetylated at lysines 5, 8, 12, and 16, methylated at arginine 3 and lysine 20, and phosphorylated at serine 1 (3, 7, 8). Unlike the dynamic process of histone acetylation and phosphorylation, histone methylation is regarded as a relatively static long-term signal with a low turnover of the methyl group. Whereas arginine can be either mono- or dimethylated (the latter in symmetric or asymmetric form), lysine methylation can occur as a mono-, di-, or trimethylated derivative. In contrast to histone H3 methylation, H4-Lys²⁰ was long considered to be maximally dimethylated in mammals (9). Most recently, however, Sarg *et al.* (10) conducted a mass spectrometric analysis with a newly developed hydrophilic interaction chromatographic method enabling the simultaneous separation of methylated and acetylated forms and, for the first time, found *in vivo* evidence that H4-Lys²⁰ is also trimethylated in mammalian tissue. Moreover, in rat liver and kidney the proportion of trimethylated histone H4 increases during aging. In Raji and K562 cells the trimethylated form was also detected, primarily when the cells were accumulated in the stationary phase (10). Most recently, two novel SET domain histone methyltransferases, Suv4-20h1 and Suv4-20h2, acting as nucleosomal H4-Lys²⁰ trimethylating enzymes, have been identified (11). It was also shown that histone H3-Lys⁹ trimethylation is required for the induction of H4-Lys²⁰ trimethylation (H4-tri-meLys²⁰) and that trimethylation of histone H3-Lys⁹ and histone H4-Lys²⁰ functions as a repressive mark in gene-silencing mechanisms (11, 12).

Studies investigating possible links between histone methylation and acetylation have revealed that methylation of Arg³ of H4 by the histone H4-specific protein methyltransferase PRMT 1 facilitates acetylation by p300 on histone H4-Lys⁸ and -Lys¹² and that this methylation at position 3 plays an important role in transcriptional regulation (7, 8). Acetylation on any of the four H4 lysines on the N-terminal tail (Lys⁵, Lys⁸, Lys¹², Lys¹⁶), however, inhibits the methylation of Arg³ by PRMT 1 (7, 8). These results demonstrate the interplay between histone

* This work was supported in part by the Oesterreichische Nationalbank, Jubilaeumsfondprojekt 9319. The costs of publication of this article were defrayed in part by the payment of page charges. This article must therefore be hereby marked "advertisement" in accordance with 18 U.S.C. Section 1734 solely to indicate this fact.

§ These authors contributed equally to this work.

|| To whom correspondence should be addressed. Tel.: 43-512-507-3521; Fax: 43-512-507-2876; E-mail: herbert.lindner@uibk.ac.at.

H4 methylation and acetylation support the histone code hypothesis. Recent findings suggest that histone H4-Lys²⁰ methylation inhibits H4-Lys¹⁶ acetylation and vice versa, leading to the hypothesis that methylation of H4-Lys²⁰ maintains silent chromatin, in part by precluding neighboring acetylation on the H4 tail (13, 14). These studies, however, did not discriminate between the individual methylation states (3–5).

Of particular interest are recent findings regarding the role of various states of histone H3/H4 methylation in the regulation of transcription. In contrast to the dimethylated state of histone H3-Lys⁴, which occurs at both inactive and active euchromatic genes, H3-Lys⁴ trimethylation is present exclusively at active genes (15), whereas H3-Lys⁹ trimethylation and also H4-Lys²⁰ trimethylation are present in repressive chromatin domains (11, 15). It is obvious, therefore, that not only methylation in itself but the precise methylation state and the position of the lysine determine gene activity/repression.

In the present study we aimed to investigate the changes in Lys²⁰ methylation states of non-, mono-, di-, tri-, and tetraacetylated H4 histones as well as the interplay between the various H4-Lys²⁰ methylation states and acetylation during *in vitro* differentiation of mouse erythroleukemia cells induced by Me₂SO¹/HMBA and the deacetylase inhibitors sodium butyrate/TSA, respectively. For the analysis we used a hydrophilic interaction liquid chromatographic method recently developed in our laboratory (2, 16–19) in combination with a mass spectrometric analysis enabling the simultaneous separation of non-, mono-, di-, and trimethylated Lys²⁰ of non-, mono-, di-, tri-, and tetraacetylated H4 histones. In all cases and regardless of the nature of the inducer we found a strong increase in the trimethylated Lys²⁰ of non- and monoacetylated histone H4 (ac0 H4-tri-meLys²⁰ and ac1 H4-tri-meLys²⁰, respectively) during differentiation. By using an antibody that specifically recognizes trimethylated Lys²⁰ of histone H4, it was possible to demonstrate that H4-tri-meLys²⁰ localizes to heterochromatin. The observed increase in non- and monoacetylated H4-tri-meLys²⁰ thus results in an increase in heterochromatic regions, thereby indicating chromatin compaction and repression of gene activity in the course of erythroid differentiation. Treatment of mouse erythroleukemia cells with sodium butyrate or TSA resulted in H4 histone hyperacetylation. With regard to the individual acetylated forms in detail, we found diacetylated H4-Lys²⁰ to be trimethylated in traces, whereas tri- and tetraacetylated H4-Lys²⁰ were not trimethylated at all. We therefore suggest that in contrast to non- and monoacetylated H4 histones, which correlate with H4-tri-meLys²⁰, histone H4 hyperacetylation precludes Lys²⁰ trimethylation, thus providing further support for the histone code hypothesis. Independently of the degree of acetylation, however, we found histone H4-dimeLys²⁰ and, to a far lesser extent, histone H4-mono-meLys²⁰.

EXPERIMENTAL PROCEDURES

Materials—Sodium perchlorate (NaClO₄), triethylamine (TEA), acetonitrile, and trifluoroacetic acid were purchased from Fluka (Buchs, Switzerland). All other chemicals were purchased from Merck (Darmstadt, Germany) if not otherwise indicated.

Cell Culture—Mouse erythroleukemia (MEL) cells (line F4N) were grown in Dulbecco's minimum Eagle's medium (Biochrom, Berlin, Germany) containing 2× nonessential amino acids, 1× penicillin-streptomycin, and 10% fetal calf serum. Cells were cultured at initial cell densities of 5.10⁴–7.10⁴/ml at 37 °C and 5% CO₂. Differentiation was

induced by the addition of 2% Me₂SO (for 144 h), 5 mM HMBA (144 h), 4 ng/ml TSA (144 h), or 1.75 mM sodium butyrate (72 h). The untreated control cells were harvested after 72 h in the log phase or after 144 h in stationary phase. The percentage of benzidine-positive cells was determined as described by Orkin *et al.* (20).

Preparations of Histones—The histones were extracted from MEL cells with sulfuric acid (0.2 M) according to the procedure of Helliger *et al.* (21).

High Performance Liquid Chromatography—The equipment used consisted of a 127 Solvent Module and a Model 166 UV-visible region detector (Beckman Instruments). The effluent was monitored at 210 nm, and the peaks were recorded using Beckman System Gold software. Solvent compositions are expressed as v/v throughout this text.

Reversed-phase HPLC—The separation of core histones was performed on a Nucleosil C₄ column (250 × 8-mm inner diameter, 5-μm particle pore size, 30-nm pore size, end-capped; Seibersdorf). Samples (~500 μg) were injected onto the column. The histone sample was chromatographed as described previously (10, 22).

Hydrophilic Interaction Liquid Chromatography—The histone fraction H4 (~100 μg) isolated by RP-HPLC was further separated on a SynChropak CM300 column (250 × 4.6-mm inner diameter, 6.5-μm particle size, 30-nm pore size; Agilent Technologies, Vienna, Austria) at 30 °C and at a constant flow of 1.0 ml/min using a multi-step gradient starting at solvent A-solvent B (100:0) (solvent A: 70% acetonitrile, 0.015 M TEA/H₃PO₄, pH = 3.0; solvent B: 65% acetonitrile, 0.015 M TEA/H₃PO₄, pH = 3.0, and 0.68 M NaClO₄). The concentration of solvent B was increased from 0 to 10% B in 2 min and from 10 to 40% in 30 min and was then maintained at 40% for 10 min. The isolated protein fractions were desalted using RP-HPLC. Histone fractions obtained in this way were collected and, after the addition of 20 μl of 2-mercaptoethanol (0.2 M), were lyophilized and stored at –20 °C.

Endoproteinase Glu-C Digestion—Histone H4 (~10 μg) obtained by HILIC fractionation was digested with *Staphylococcus aureus* V8 protease (Roche Applied Science; 1:20 w/w) in 50 μl of 25 mM NH₄HCO₃ buffer (pH 4.0) for 1 h at room temperature. The digest was subjected to RP-HPLC as described previously (10).

Endoproteinase Lys-C Digestion—N-terminal peptides obtained by Glu-C digestion were further cleaved with endoproteinase Lys-C (Roche Applied Science; 1:5 w/w) in 15 μl of 25 mM Tris-HCl buffer (pH 8.7) for 2 h at 37 °C. The digest was subjected to RP-HPLC-ESI-MS.

Mass Spectrometric Analysis—Histone H4 peptide fractions obtained by endoproteinase Lys-C cleavage were injected onto a PepMap C₁₈ column (150 × 1-mm inner diameter, 3-μm particle size; ICT, Vienna, Austria). The column eluate was coupled directly to a Finnigan LCQ ion trap instrument (San Jose, CA) equipped with an electrospray source (RP-HPLC-ESI-MS). Samples of ~1 μg were chromatographed within 55 min at a constant flow of 35 μl/min with a two-step acetonitrile gradient starting at solvent A – solvent B (90:10) (solvent A: water containing 0.1% trifluoroacetic acid; solvent B: 85% acetonitrile and 0.093% trifluoroacetic acid). The concentration of solvent B was increased linearly from 10 to 40% over a 45-min period and from 40 to 100% over 20 min.

Antibodies—The antibodies used were: rabbit polyclonal to H4-tri-meLys²⁰ (Abcam), Western blotting 1:1000, immunofluorescence 1:200; rat monoclonal to HP1β (Abcam), immunofluorescence 1:50; mouse monoclonal to RNA polymerase II (Abcam), immunofluorescence 1:50. For Western blotting, goat anti-rabbit IgG peroxidase conjugate (Sigma) 1:5000 was used as secondary antibody. The secondary antibodies for immunofluorescence were: goat anti-rabbit IgG fluorescein isothiocyanate conjugate (Sigma), 1:160; goat anti-rat IgG Cy3 conjugate (Jackson ImmunoResearch), 1:160; goat anti-mouse IgG Cy3 conjugate (Jackson ImmunoResearch), 1:160.

Western Blotting—Histones were resolved in SDS-loading buffer, fractionated by SDS-PAGE, and transferred to a nitrocellulose membrane (Hybond ECL, Amersham Biosciences). The membrane was probed with antibodies using standard techniques and detected by enhanced chemiluminescence (ECL, Amersham Biosciences).

Immunofluorescence—MEL cells were grown in suspension culture, collected by centrifugation, and washed with phosphate-buffered saline. 10⁶ cells were cytospun onto slides. Cells were permeabilized using Triton X-100 (1% for 2 min and 0.1% for 10 min) in KCM buffer (120 mM KCl, 20 mM NaCl, 0.5 mM EDTA, 10 mM Tris/HCl, pH 7.5) and incubated sequentially with the primary and secondary antibodies. Cells were fixed for 5 min with 4% paraformaldehyde in KCM, stained with DAPI for 1 min, and mounted in mounting medium (Dako). Staining was visualized using an ×100 objective on a Zeiss Axioplan 2 microscope and a SPOT camera (Diagnostic Instruments). Images were captured using MetaVue software (Universal Imaging Corp.) and analyzed with Corel Photo-Paint 10.

¹ The abbreviations used are: Me₂SO, dimethyl sulfoxide; DAPI, 4,6-diamidino-2-phenylindole; ESI-MS, electrospray ionization mass spectrometry; HDAC, histone deacetylase; HILIC, hydrophilic interaction liquid chromatography; HMBA, hexamethylenebisacetamide; HP1, heterochromatin protein-1; MEL, mouse erythroleukemia; RP-HPLC, reversed-phase high performance liquid chromatography; TEA, triethylamine; TSA, trichostatin A.

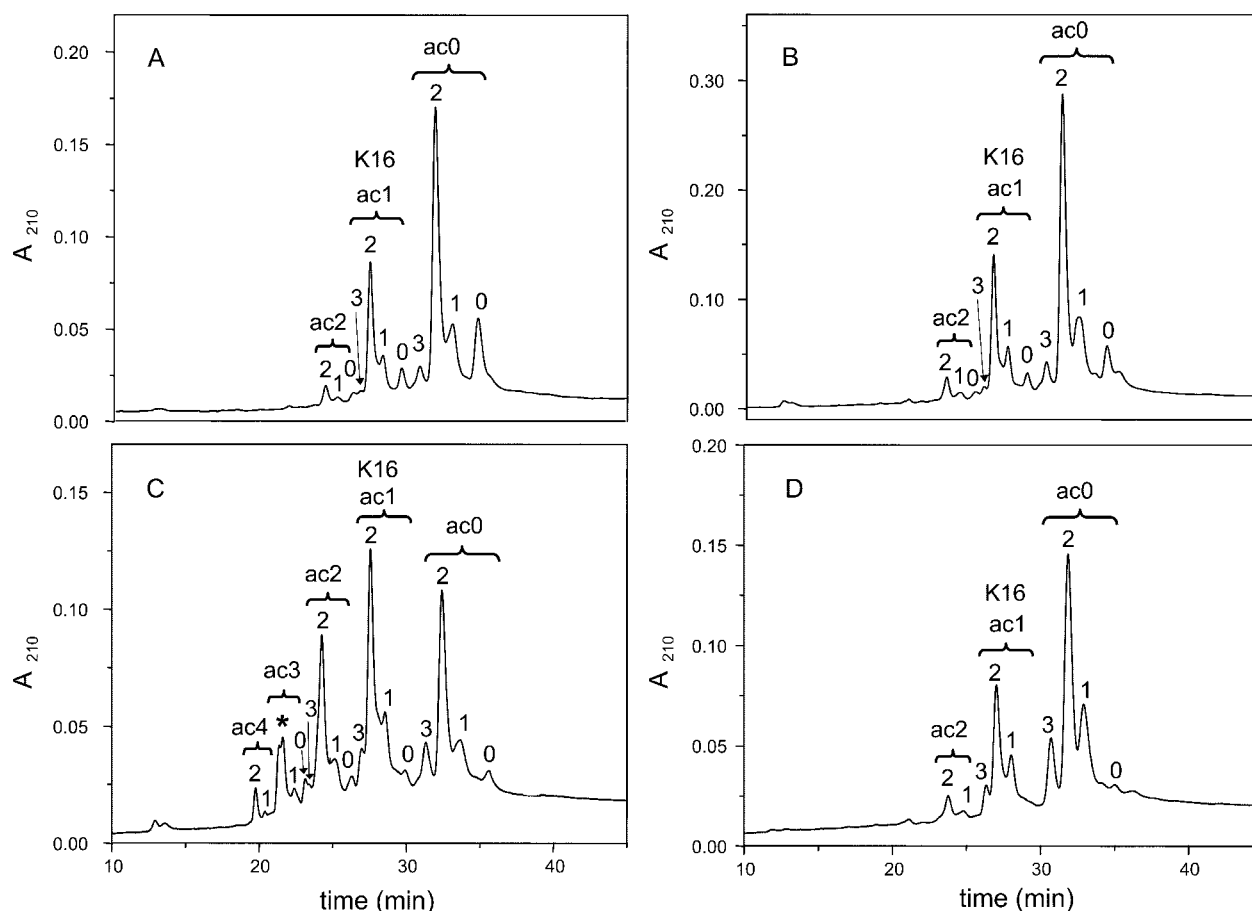


FIG. 1. HILIC separation of histone H4 of uninduced MEL cells and cells cultured in the presence of sodium butyrate and Me₂SO. The histone H4 fractions were analyzed on a SynChropak CM300 column (250 × 4.6 mm) at 30 °C at a constant flow of 1.0 ml/min using a two-step gradient starting at 100% A, 0% B (solvent A: 70% acetonitrile, 0.015 M TEA/H₃PO₄, pH = 3.0; solvent B: 65% acetonitrile, 0.015 M TEA/H₃PO₄, pH 3.0, and 0.68 M NaClO₄). The concentration of solvent B was increased from 0 to 10% B for 2 min and from 10 to 40% for 30 min and then was maintained at 40% for 10 min. *A*, untreated (control) MEL cells 72 h; *B*, 144 h after seeding (~100 μg of H4). *C*, cells grown for 72 h in the presence of butyrate (~300 μg of H4). *D*, cells grown for 144 h in the presence of Me₂SO (~100 μg of H4). The isolated protein fractions (designated ac0–ac4 for the non-, mono-, di-, tri-, and tetraacetylated forms and 0–3 for the non-, mono-, di-, and trimethylated forms) were desalted using RP-HPLC. Histone fractions obtained in this way were collected and then, after the addition of 20 μl of 2-mercaptoethanol (0.2 M), were lyophilized and stored at –20 °C.

RESULTS

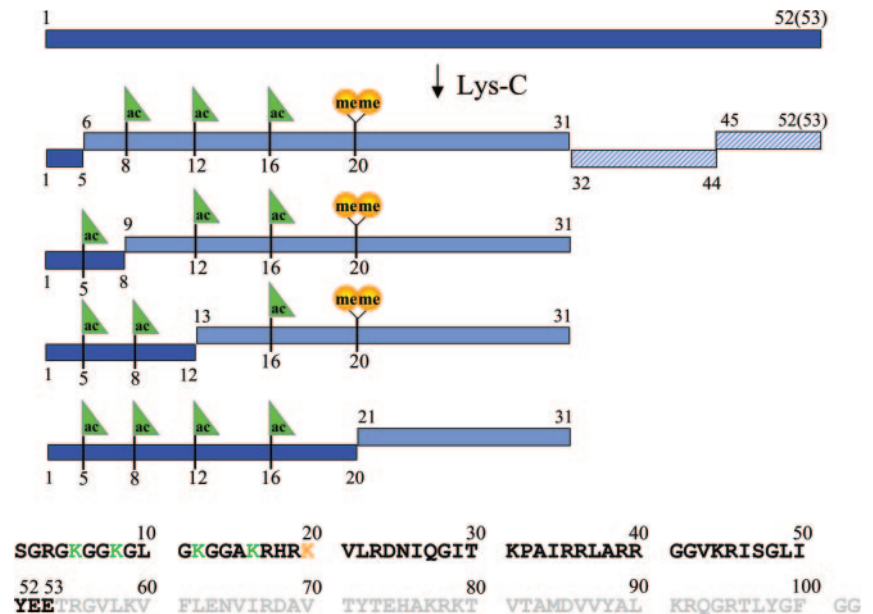
HILIC Separation of Modified Forms of Histone H4 of Uninduced MEL Cells and Cells Cultured in the Presence of Me₂SO, HMBA, Sodium Butyrate, and TSA—Untreated MEL cells and cells treated with Me₂SO, HMBA, sodium butyrate, and TSA were grown in culture. After 72 and 144 h and before harvesting the cells, the number of benzidine-positive cells indicating hemoglobin accumulation was determined. In the case of butyrate-treated cells, however, the study was limited to the first 72 h, because butyrate is metabolized by the cells, and after a certain time its concentration is reduced to a level below that required to stimulate differentiation (23). Whereas throughout the entire period study untreated cultures were found to contain a very low level (less than 2%) of spontaneously differentiated cells, cultures containing Me₂SO, HMBA, or butyrate produced ~80–95% benzidine-positive cells and those containing TSA nearly 70%.

The sulfuric acid-extracted core histones were fractionated using an RP-HPLC procedure described previously (10, 22), and the histone H4 fractions obtained were subjected to HILIC, a chromatographic technique developed in our laboratory for separating modified core and H1 histones (2, 16–19). A number of major and minor peaks could be received, which were identified by ESI-MS as described previously (10). Fig. 1 shows the pattern of histone H4 acetylation and methylation of untreated (control) MEL cells at 72 h (Fig. 1A) and 144 h (Fig. 1B) after

seeding, respectively, and of cells grown for 72 h in the presence of butyrate (Fig. 1C) and 144 h in the presence of Me₂SO (Fig. 1D). The histone H4 acetylation/methylation pattern of MEL cells grown for 144 h in the presence of TSA and HMBA resembled that obtained by treating with butyrate and Me₂SO, respectively (data not shown). In control cells and cells treated with Me₂SO and HMBA, histone H4 was hypoacetylated, containing primarily non acetylated (ac0) and monoacetylated (ac1) forms with Lys¹⁶ as the most frequently acetylated lysine residue. In response to Me₂SO treatment, a clear increase in trimethylated unacetylated and trimethylated monoacetylated H4 species was observed (Fig. 1, *D* versus *B*). Treatment of cells with butyrate and TSA, known HDAC inhibitors, caused hyperacetylation of H4, in which up to four acetyl groups are bound to the N-terminal tail. The results revealed that H4-Lys²⁰ is methylated in all of the acetylated isoforms, as well as in the nonacetylated isoform, apart from a nonmethylated H4 present in varying amounts. In general, the dimethylated form was found to be the main methylation product followed, in smaller amounts, by the mono- and trimethylated forms. To facilitate an unambiguous assignment, the double peak of triacetylated H4 histones (designated in Fig. 1C with an asterisk) had to be investigated in more detail.

Characterization of Hyperacetylated H4 Fractions from Butyrate-treated Cells Obtained by HILIC—To precisely deter-

FIG. 2. Peptide patterns obtained after endoproteinase Glu-C and Lys-C digestion of HILIC-Peak ac3 (marked with an asterisk). The peak marked with an asterisk, which was obtained from butyrate-treated MEL cells by HILIC (Fig. 1C), was digested with endoproteinase Glu-C. The resulting peptide fractions were separated using RP-HPLC (data not shown). The blocked N terminus (residues 1–52, 1–53) obtained was further digested by Lys-C. The resulting peptides and their attached modifications were identified using ESI-MS. Mouse histone H4 sequence data were taken from the Swiss Protein Database (accession number P02304).



mine the modification status of hyperacetylated histone H4 shown in Fig. 1C, the HILIC fractions were isolated, desalted by RP-HPLC, and treated with endoproteinase Glu-C as described previously (10). The fragmentation yielded an N-terminal peptide (residues 1–52 and 1–53) that was further cleaved with endoproteinase Lys-C. Endoproteinase Lys-C is a serine protease, and its activity is inhibited at lysine residues that have been modified by an acetyl or methyl group (10). The digests were analyzed by RP-HPLC-ESI-MS using a 150 × 1.0-mm inner diameter microbore column. The diacetylated (ac₂) form was found to be acetylated at Lys¹⁶ and Lys¹², and as can be seen from the separation pattern in Fig. 1C, was mainly dimethylated followed by the monomethylated derivative and, present in trace amounts only, the trimethylated one. In the case of the triacetylated H4 protein (marked with an asterisk), which is separated into two HILIC subfractions, several peptide fragments were detected (Fig. 2). ESI-MS analysis revealed a triacetylated H4-di-meLys²⁰ form with acetyl groups at either Lys⁸-Lys¹²-Lys¹⁶ or Lys⁵-Lys¹²-Lys¹⁶ and, in very small amounts, at Lys⁵-Lys⁸-Lys¹⁶. This finding that the various lysines are partially occupied in the triacetylated form agrees well with observations made by other investigators (24, 25). Interestingly, a peptide corresponding to the tetraacetylated (Lys⁵-Lys⁸-Lys¹²-Lys¹⁶) nonmethylated form, which could not be separated by the HILIC system, was found in the ac₃ double peak. A triacetylated trimethylated H4 histone, however, was undetectable. Concerning the tetraacetylated H4 protein, two HILIC subfractions containing one or two methyl groups were identified. Similar to triacetylated H4, a tetraacetylated trimethylated H4 was also not seen. At any rate, however, the H4-di-meLys²⁰ form predominates in the hyperacetylated histone H4 fractions.

The Levels of H4-tri-meLys²⁰ Are Raised in Hypoacetylated H4 Fractions during MEL Cell Differentiation—We recently showed for the first time that histone H4 from mammalian tissue is not only mono- and dimethylated but also trimethylated at Lys²⁰ and that the trimethylated form accumulates with age and in cells in the stationary phase (10). Novel studies on methylated histones have revealed that H4-tri-meLys²⁰ is a repressive mark in gene silencing and is important for heterochromatin assembly (11, 12). We were thus interested in investigating the occurrence of trimethylated H4 in differentiated cells. To obtain quantitative data, we conducted a HILIC analysis of histone H4 from MEL cells treated with various induc-

ers and quantified the results. As depicted in Fig. 3A, an increase of about 70% in trimethylated H4 (ac₀ + ac₁) forms appears in non-growing cells. Upon induction a remarkable further increase to the 4–5-fold level occurs in differentiated cells. In addition, using an anti-H4-tri-meLys²⁰ antibody we investigated the level of H4-tri-meLys²⁰ in cells treated with Me₂SO for 96 h (Fig. 3B, lane 4) and in untreated control cells (Fig. 3B, lane 3). In Me₂SO-induced cells we found an H4-tri-meLys²⁰-increase similar to that observed in HILIC (Fig. 3A). Fig. 3C shows the relative amount of H4-tri-meLys²⁰ from the nonacetylated fraction in comparison with the monoacetylated one. Besides the increase in H4-tri-meLys²⁰ in both the ac₀ and ac₁ fraction of treated and untreated cells, it is obvious that the proportion of trimethylation is always about 2-fold higher in nonacetylated than in monoacetylated H4. Nishioka *et al.* (13) found that in *Drosophila*, methylation of H4-Lys²⁰ and acetylation of Lys¹⁶ are competitive. We favor the view that not methylation in itself but the degree of methylation plays a role in that interplay and that acetylated H4-Lys¹⁶ does not influence mono- or dimethylation but reduces trimethylation of H4-Lys²⁰. It is also interesting to note that in non- and monoacetylated H4 with increasing trimethylation we saw a decreasing amount of H4-non-meLys²⁰ (designated as 0 in Fig. 1). This observation is in line with the *in vitro* finding that Suv4-20h is a Lys²⁰ trimethylase preferring nonmethylated H4 as substrate (11).

H4-tri-meLys²⁰ Localizes to Heterochromatin—To investigate the localization and distribution of H4-tri-meLys²⁰ in chromatin of untreated control and differentiated MEL cells we used indirect immunofluorescence analysis (Fig. 4). Generally, during *in vitro* differentiation of MEL cells, their nuclei were reduced in volume and the chromatin appeared to be highly compacted (Fig. 4, lower row in both A and B, DAPI stain). Important markers of condensed DNA, which are key components of constitutive heterochromatin, represent the heterochromatin proteins HP1 α and HP1 β (26). We found that H4-tri-meLys²⁰ was enriched mainly within DAPI-dense regions, which almost completely overlap with HP1 β -stained chromatin regions both in control and in Me₂SO-treated cells (Fig. 4A). To verify this finding and to exclude any association between H4-tri-meLys²⁰ and transcriptionally engaged chromatin, dual staining experiments were performed using the H4-tri-meLys²⁰-specific antibody and an antibody against RNA polymerase II (27). We found that the majority of H4-tri-meLys²⁰ is

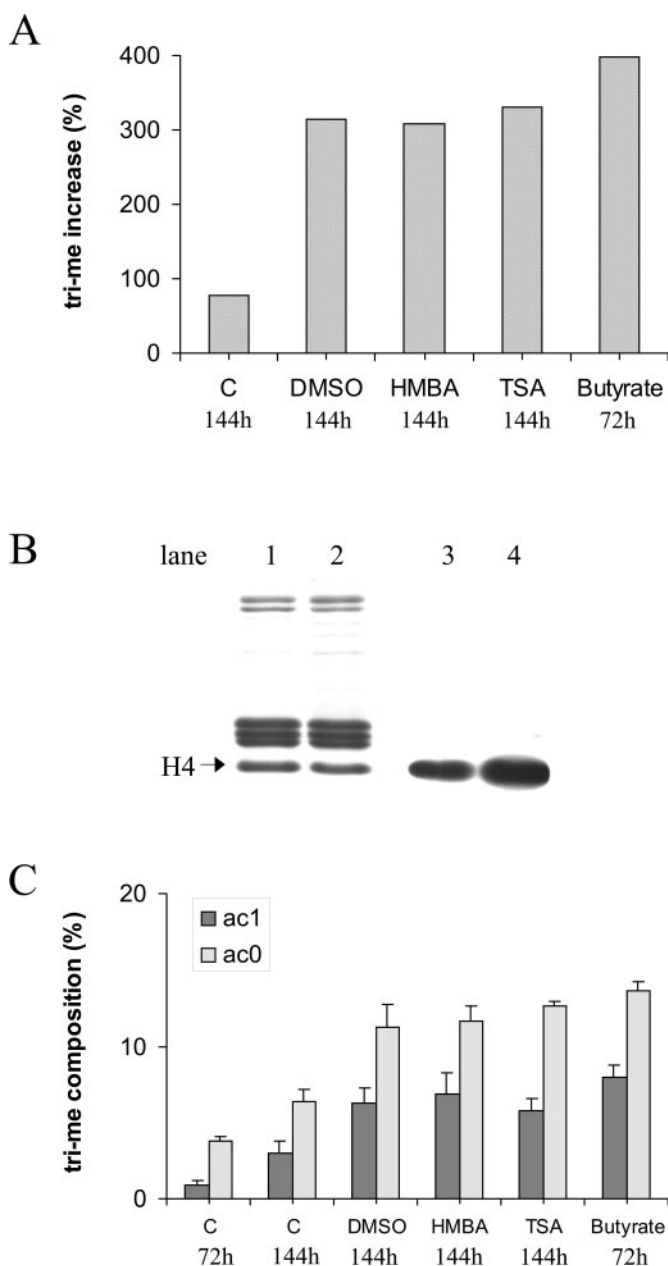


FIG. 3. Increase of H4-tri-meLys²⁰ of hypoacetylated (ac0 + ac1) forms during MEL cell differentiation. A, H4 was obtained from untreated (control) MEL cells 72 and 144 h after seeding and from cells grown for 72 h in the presence of butyrate and for 144 h in the presence of dimethyl sulfoxide (DMSO), HMBA, and TSA. The H4 fractions (~100–300 μ g) isolated with RP-HPLC were analyzed under the same HILIC conditions described in the legend for Fig. 1. The amount of H4-tri-meLys²⁰ was quantified using Beckman System Gold software. The relative increase in H4 trimethylation of nongrowing cells and induced cells was compared with the 72-h control (0%). B, MEL cells were cultured for 96 h in normal culture medium (lanes 1 and 3) or in culture medium containing 2% dimethyl sulfoxide (lanes 2 and 4). Histones from the two cell samples were separated by SDS-PAGE, blotted, and probed with H4-tri-meLys²⁰ polyclonal antibody. Lanes 1 and 2 show a Coomassie Blue-stained profile of the samples used in the immunoblot (lanes 3 and 4). C, same conditions as described in A. The relative amount of nonacetylated (ac0) H4-Lys²⁰ trimethylation was compared with the monoacetylated (ac1) trimethylated form. Results represent means \pm S.D. for three to five independent experiments.

largely excluded from active chromatin regions, thus indicating an association with transcriptionally silent chromatin (Fig. 4B). Our investigations therefore have demonstrated that H4-tri-meLys²⁰ is largely localized within distinct domains of constitutive heterochromatin both in untreated MEL cells, which

accumulate in the stationary phase, and in MEL cells induced to differentiate.

Histone H4 Hyperacetylation Precludes H4-Lys²⁰ Trimethylation—Histone hypoacetylation and methylation are involved in gene silencing (5), whereas histone acetylation is associated with transcriptionally active genes (28). Therefore, we were interested in examining the methylation status of hypo- and hyperacetylated H4 proteins. Table I shows a summary of the various methylation patterns of histone H4 from undifferentiated (control) MEL cells (72 and 144 h) and from differentiated cells grown in the presence of Me₂SO, HMBA, butyrate or TSA. As shown in Table I, the H4-Lys²⁰ methylation status from hypoacetylated forms ac0 and ac1 did not differ between undifferentiated and differentiated cells, namely mono-me-, di-me-, and tri-meH4-Lys²⁰ were found in each of them. Concerning the diacetylated H4 fraction, the smallest traces of H4-tri-meLys²⁰ might have been present in some samples treated with Me₂SO, HMBA, and TSA. Minimal but detectable amounts, however, were present in samples from butyrate-treated cells. The mono- and dimethylated form of Lys²⁰ was also seen in the hyperacetylated histone H4 fractions, but trimethylated Lys²⁰ was not detected in the tri- and tetraacetylated proteins. As mentioned before, Lys¹⁶ acetylation causes a decrease in Lys²⁰ trimethylation, whereas hyperacetylation with further acetyl groups at Lys¹², Lys⁸, and/or Lys⁵ even causes a complete repression of H4-Lys²⁰ trimethylation.

DISCUSSION

In this study we aimed to quantify the changes in histone H4 methylation and acetylation levels in the course of *in vitro* differentiation of mouse erythroleukemia cells and to investigate their consequences regarding heterochromatin formation. Using a polar stationary phase in the presence of acetonitrile, unmodified H4 and its differently acetylated/methylated forms were separated from each other due to slight variations in the polarity of the proteins caused by the modification reactions. To emphasize the polar nature of intermolecular forces governing retention with such stationary phases, the term hydrophilic interaction chromatography, with the acronym HILIC, was suggested by Alpert (29). This HILIC-MS technique applied has a series of advantages over immunoassays now commonly used in this field. First, the whole histone H4 acetylation and methylation pattern is obtained not only simultaneously but also in extreme detail. In addition, the method requires only small sample amounts and gives results within 35 min.

When untreated cells were accumulated in the stationary phase, the proportion of non- and monoacetylated H4-tri-meLys²⁰ increased modestly, whereas in particular that of the nonacetylated H4-non-meLys²⁰ but also of the monoacetylated H4-non-meLys²⁰ form decreased (Fig. 1, A and B). When MEL cells were induced with Me₂SO, HMBA, butyrate, or TSA, we observed an impressive increase in non- and monoacetylated H4-tri-meLys²⁰, indicating that H4-Lys²⁰ trimethylase Suv4-20h activity increases as cells are induced. Using immunofluorescence we demonstrated that H4-tri-meLys²⁰ localizes to heterochromatin, and thus the ratio of heterochromatin rises in the course of differentiation and, to a minor extent, when untreated exponentially growing cells reach the stationary phase. In this context it should be mentioned that a similar accumulation of heterochromatin structure was also found in senescent human fibroblasts (30). When the cells were induced with deacetylase inhibitors (butyrate or TSA), we found non- and monoacetylated H4 histones, which were definitely trimethylated at Lys²⁰. However, the diacetylated H4 histones were hardly, and the tri- and tetraacetylated ones were absolutely not trimethylated. We thus conclude that H4-Lys²⁰ trimethylation is maximally compatible only with nonacetylated

FIG. 4. Co-immunostaining of differentiated (treatment with dimethyl sulfoxide for 96 h) and untreated (Control) MEL cells using antibodies that detect HP1 β , RNA polymerase II, and H4-tri-meLys²⁰. *A*, distribution of HP1 β (red), which detects heterochromatic sites, and H4-tri-meLys²⁰ (green) in mouse MEL nuclei. In the far right column, the HP1 β (Cy3, red) and H4-tri-meLys²⁰ (FITC, green) staining patterns were visualized simultaneously (*Merge*). DNA was counterstained with DAPI to highlight the foci of heterochromatin. *B*, distribution of RNA polymerase II (red), which detects transcriptionally competent regions, and H4-tri-meLys²⁰ (green) in MEL nuclei. In the far right column, the polymerase II (Cy3, red) and H4-tri-meLys²⁰ (FITC, green) staining patterns were visualized simultaneously (*Merge*). DNA was counterstained with DAPI to highlight the foci of heterochromatin. Scale bars, 5 μ m.

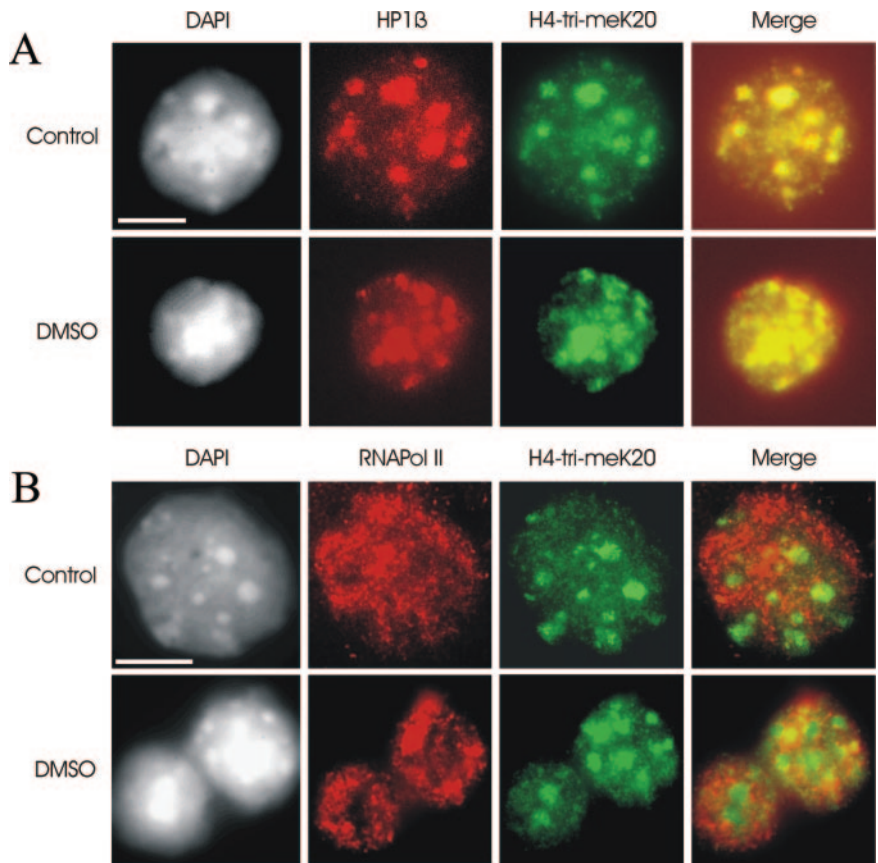


TABLE I
Acetylation/methylation status of histone H4

A summary of the occurrence of various acetylated and methylated forms in untreated (control) cells and cells treated with several inducers is shown. Results show the presence (+) or absence (-) of mono-, di-, or trimethylated H4-Lys²⁰ in the various acetylated H4 proteins.

H4	Controls	Me ₂ SO/HMBA	Butyrate/TSA
ac0			
mono-me	+	+	+
di-me	+	+	+
tri-me	+	+	+
ac1			
(Lys ¹⁶)			
mono-me	+	+	+
di-me	+	+	+
tri-me	+	+	+
ac2			
(Lys ¹⁶ ,Lys ¹²)			
mono-me	+	+	+
di-me	+	+	+
tri-me	-	-	(+)
ac3			
(Lys ¹⁶ ,Lys ¹² ,Lys ⁸)			
(Lys ¹⁶ ,Lys ¹² ,Lys ⁵)			
(Lys ¹⁶ ,Lys ⁸ ,Lys ⁵)			
mono-me	-	-	+
di-me	-	-	+
tri-me	-	-	-
ac4			
(Lys ¹⁶ ,Lys ¹² ,Lys ⁸ ,Lys ⁵)			
mono-me	-	-	+
di-me	-	-	+
tri-me	-	-	-

and, to a lesser degree, monoacetylated histone H4 and that H4 hyperacetylation and Lys²⁰ trimethylation preclude one another completely. This result is consistent with earlier studies demonstrating that H4 methylation preferentially occurs on unacetylated histones (9). It should be pointed out, however,

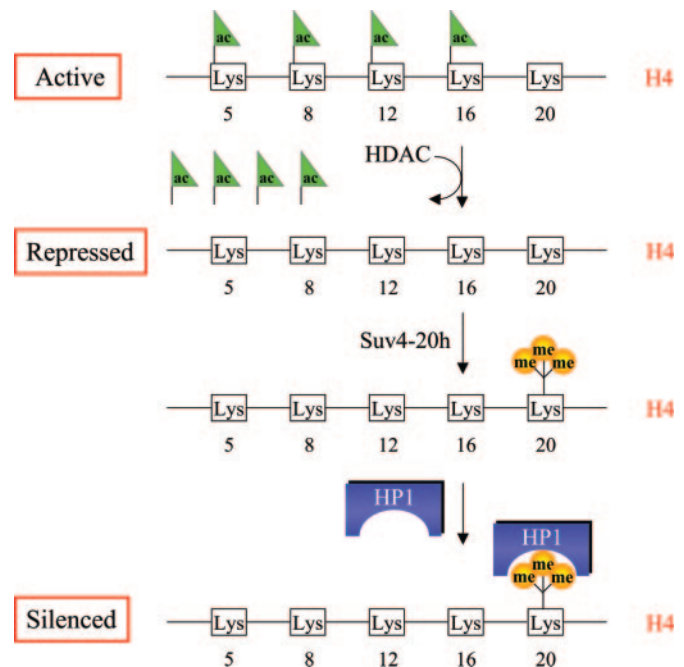


FIG. 5. A proposed model for how epigenetic modifications might cause gene silencing. HDAC deacetylates lysines 5, 8, 12, and 16 in the N-terminal tail of histone H4, which can in turn be trimethylated at Lys²⁰ by Suv4-20h. Trimethylated H4-Lys²⁰ is recognized by HP1, resulting in the maintenance of gene silencing.

that the mutual inducement observed solely concerns the interplay between hyperacetylation and Lys²⁰ trimethylation but not between hyperacetylation and Lys²⁰ mono- or dimethylation. In fact, we found non-, mono-, di-, tri-, and tetraacetylated H4 histones that were mono- and dimethylated. This outcome also agrees well with the finding that H4-di-meLys²⁰ is broadly

distributed in euchromatin (11).

The fact that certain combinations of acetyl and methyl modifications of lysines in histone tails may have antagonistic or cooperative biological effects is repeatedly described in the literature (7, 9, 13, 14, 31–36). Although acetylation at Lys⁹ in histone H3 prevents methylation of that amino acid (37), acetylation at any of the four lysines (Lys⁵, Lys⁸, Lys¹², Lys¹⁶) of histone H4 inhibits Arg³ methylation, whereby acetylation at Lys⁵ has the greatest effect (7). In this context it should be mentioned that our study detected no methylation of H4-Arg³. Nishioka *et al.* (13) described the identification and characterization of a mammalian histone methyltransferase, PR-Set7, which specifically methylates the Lys²⁰ of histone H4. In *in vitro* experiments these authors (13) demonstrated that methylation at H4-Lys²⁰ inhibits the acetylation of H4-Lys¹⁶ and that, vice versa, acetylation of H4-Lys¹⁶ precludes methylation of the neighboring Lys²⁰. The acetylation of Lys¹², however, was not found to be inhibited by Lys²⁰ methylation. In this context it should be noted that the investigations of Nishioka *et al.* (13) were performed using dimethylated H4-Lys²⁰, whereas our study revealed the interactions between acetylation and mono-, di-, and trimethylation of H4-Lys²⁰.

The mechanisms by which euchromatin is converted to heterochromatin are still unknown. Based on the results obtained in our study, we propose a model showing how epigenetic modifications might convert unmethylated “active” chromatin into trimethylated “silenced” chromatin (Fig. 5). The first step involves the deacetylation of hyperacetylated H4 by specific HDACs. Thereafter, the unmodified histone H4 is trimethylated at Lys²⁰ by a Suv4-20h methylase. If there exists an Suv4-20h-HDAC multienzyme complex similar to the SU(VAR)3-9-HDAC1 protein complex present in *Drosophila* histone H3 (31), it would also be imaginable that deacetylation and trimethylation occur in a concerted manner. In the subsequent last step, HP1 binds to the H4-tri-meLys²⁰, which in turn causes chromatin compaction.

Histone modifications and DNA methylation are the major epigenetic mechanisms that can effect gene expression in mammals (38). Recent studies indicate a connection between histone H3 and DNA methylation (39–42). Tamaru *et al.* (41) suggested that H3-tri-meLys⁹ affects DNA methyltransferases, causing cytosine methylation on nearby DNA. The observations support the idea that histone H3 and DNA methylation cooperate in establishing long-term states of transcriptional regulation. Because H3-Lys⁹ and H4-Lys²⁰ trimethylation have the same functional consequences, we also assume an interaction between H4-tri-meLys²⁰ and DNA methyltransferases.

It is known that DNA hypermethylation and histone deacetylation are involved in tumor suppressor gene silencing in cancer (41, 43, 44). For this reason, inhibitors of histone deacetylases, such as TSA, have great potential for the treatment of malignant disease (45). Recently, it was shown that histone H3-Lys⁹ methylation/acetylation also has a crucial function in epigenetic regulation of suppressor genes: combined treatment with TSA and a DNA methyltransferase inhibitor resulted in an increase in H3-Lys⁹ acetylation and a simultaneous decrease in histone H3-Lys⁹ methylation, correlating with re-expression of silenced suppressor genes (43, 44). We surmise that there is a similar TSA effect on histone H4. As our study shows, TSA, similar to sodium butyrate, causes H4 hyperacetylation, which prevents Lys²⁰ trimethylation and then heterochromatin formation. In this context it would be interesting to know whether a H4 trimethyltransferase inhibitor would intensify the efficacy of deacetylase inhibitors.

Acknowledgments—We thank A. Devich, S. Reichegger, B. Schimpfössl, and Dr. M. Rittinger for excellent technical assistance.

REFERENCES

- van Holde, K. E. (1988) in *Chromatin* (Rich, A., ed) Springer Series in Molecular Biology, pp. 111–148, Springer, New York
- Lindner, H., Sarg, B., Hoertnagl, B., and Helliger, W. (1998) *J. Biol. Chem.* **273**, 13324–13330
- Strahl, B. D., and Allis, C. D. (2000) *Nature* **403**, 41–45
- Turner, B. M. (2000) *BioEssays* **22**, 836–845
- Jenuwein, T., and Allis, C. D. (2001) *Science* **293**, 1074–1080
- Schneider, R., Bannister, A. J., and Kouzarides, T. (2002) *Trends Biochem. Sci.* **27**, 396–402
- Wang, H., Huang, Z. Q., Xia, L., Feng, Q., Erdjument-Bromage, H., Strahl, B. D., Briggs, S. D., Allis, C. D., Wong, J., Tempst, P., and Zhang, Y. (2001) *Science* **293**, 853–857
- Strahl, B. D., Briggs, S. D., Brame, C. J., Caldwell, J. A., Koh, S. S., Ma, H., Cook, R. G., Shabanowitz, J., Hunt, D. F., Stallcup, M. R., and Allis, C. D. (2001) *Curr. Biol.* **11**, 996–1000
- Annunziato, A. T., Eason, M. B., and Perry, C. A. (1995) *Biochemistry* **34**, 2916–2924
- Sarg, B., Koutzamani, E., Helliger, W., Rundquist, I., and Lindner, H. H. (2002) *J. Biol. Chem.* **277**, 39195–39201
- Schotta, G., Lachner, M., Sarma, K., Ebert, A., Sengupta, R., Reuter, G., Reinberg, D., and Jenuwein, T. (2004) *Genes Dev.* **18**, 1251–1262
- Kourmouli, N., Jeppesen, P., Mahadevaiah, S., Burgoyne, P., Wu, R., Gilbert, D. M., Bongiorno, S., Pranter, G., Fanti, L., Pimpinelli, S., Shi, W., Fundele, R., and Singh, P. B. (2004) *J. Cell Sci.* **117**, 2491–2501
- Nishioka, K., Rice, J. C., Sarma, K., Erdjument-Bromage, H., Werner, J., Wang, Y., Chuikov, S., Valenzuela, P., Tempst, P., Steward, R., Lis, J. T., Allis, C. D., and Reinberg, D. (2002) *Mol. Cell* **9**, 1201–1213
- Rice, J. C., Nishioka, K., Sarma, K., Steward, R., Reinberg, D., and Allis, C. D. (2002) *Genes Dev.* **16**, 2225–2230
- Santos-Rosa, H., Schneider, R., Bannister, A. J., Sherriff, J., Bernstein, B. E., Emre, N. C., Schreiber, S. L., Mellor, J., and Kouzarides, T. (2002) *Nature* **419**, 407–411
- Sarg, B., Helliger, W., Hoertnagl, B., Puschedorf, B., and Lindner, H. (1999) *Arch. Biochem. Biophys.* **372**, 333–339
- Lindner, H., Sarg, B., Meraner, C., and Helliger, W. (1996) *J. Chromatogr. A* **743**, 137–144
- Lindner, H., Sarg, B., and Helliger, W. (1997) *J. Chromatogr. A* **782**, 55–62
- Lindner, H., and Helliger, W. (2004) *Methods Mol. Biol.* **251**, 75–88
- Orkin, S. H., Harosi, F. I., and Leder, P. (1975) *Proc. Natl. Acad. Sci. U. S. A.* **72**, 98–102
- Helliger, W., Lindner, H., Grubl-Knosp, O., and Puschedorf, B. (1992) *Biochem. J.* **288**, 747–751
- Lindner, H., Helliger, W., and Puschedorf, B. (1988) *J. Chromatogr.* **450**, 309–316
- Friend, C., Zajac-Kaye, M., Holland, J. G., and Pogo, B. G. (1987) *Cancer Res.* **47**, 378–382
- Turner, B. M., O'Neill, L. P., and Allan, I. M. (1989) *FEBS Lett.* **253**, 141–145
- Clarke, D. J., O'Neill, L. P., and Turner, B. M. (1993) *Biochem. J.* **294**, 557–561
- Peters, A. H., Mermoud, J. E., O'Carroll, D., Pagani, M., Schweizer, D., Brockdorff, N., and Jenuwein, T. (2002) *Nat. Genet.* **30**, 77–80
- Kristjohan, A., Wittschieben, B. O., Walker, J., Roberts, D., Cairns, B. R., and Svejstrup, J. Q. (2003) *Proc. Natl. Acad. Sci. U. S. A.* **100**, 7551–7556
- Hebbes, T. R., Thorne, A. W., and Crane-Robinson, C. (1988) *EMBO J.* **7**, 1395–1402
- Alpert, A. J. (1990) *J. Chromatogr.* **499**, 177–196
- Narita, M., Nunez, S., Heard, E., Narita, M., Lin, A. W., Hearn, S. A., Spector, D. L., Hannon, G. J., and Lowe, S. W. (2003) *Cell* **113**, 703–716
- Czermin, B., and Imhof, A. (2003) *Genetica* **117**, 159–164
- Hake, S. B., Xiao, A., and Allis, C. D. (2004) *Br. J. Cancer* **90**, 761–769
- Schubeler, D., MacAlpine, D. M., Scalzo, D., Wirbelauer, C., Kooperberg, C., van Leeuwen, F., Gottschling, D. E., O'Neill, L. P., Turner, B. M., Delrow, J., Bell, S. P., and Groudine, M. (2004) *Genes Dev.* **18**, 1263–1271
- Rice, J. C., and Allis, C. D. (2001) *Curr. Opin. Cell Biol.* **13**, 263–273
- Zhang, Y., and Reinberg, D. (2001) *Genes Dev.* **15**, 2343–2360
- Li, J., Lin, Q., Yoon, H. G., Huang, Z. Q., Strahl, B. D., Allis, C. D., and Wong, J. (2002) *Mol. Cell Biol.* **22**, 5688–5697
- Rea, S., Eisenhaber, F., O'Carroll, D., Strahl, B. D., Sun, Z. W., Schmid, M., Opravil, S., Mechtler, K., Ponting, C. P., Allis, C. D., and Jenuwein, T. (2000) *Nature* **406**, 593–599
- Wolffe, A. P., and Matzke, M. A. (1999) *Science* **286**, 481–486
- Lehnertz, B., Ueda, Y., Derijck, A. A., Braunschweig, U., Perez-Burgos, L., Kubicek, S., Chen, T., Li, E., Jenuwein, T., and Peters, A. H. (2003) *Curr. Biol.* **13**, 1192–1200
- Xin, Z., Tachibana, M., Guggiari, M., Heard, E., Shinkai, Y., and Wagstaff, J. (2003) *J. Biol. Chem.* **278**, 14996–15000
- Tamaru, H., Zhang, X., McMillen, D., Singh, P. B., Nakayama, J., Grewal, S. I., Allis, C. D., Cheng, X., and Selker, E. U. (2003) *Nat. Genet.* **34**, 75–79
- Geiman, T. M., and Robertson, K. D. (2002) *J. Cell. Biochem.* **87**, 117–125
- Kondo, Y., Shen, L., and Issa, J. P. (2003) *Mol. Cell Biol.* **23**, 206–215
- Fujii, S., Luo, R. Z., Yuan, J., Kadota, M., Oshimura, M., Dent, S. R., Kondo, Y., Issa, J. P., Bast, R. C., Jr., and Yu, Y. (2003) *Hum. Mol. Genet.* **12**, 1791–1800
- Marks, P. A., Rifkin, R. A., Richon, V. M., and Breslow, R. (2001) *Clin. Cancer Res.* **7**, 759–760